

Collapse and revival for a slightly anharmonic Hamiltonian

Alexandra Bakman, Hagar Veksler and Shmuel Fishman

July 31, 2018

Technion - Israel Institute of Technology, Technion City, Haifa 3200003, Israel

Abstract

The effect of quantum collapse and revival is a fascinating interference phenomenon. In this paper the phenomenon is demonstrated analytically and numerically for a simple system, a slightly anharmonic Hamiltonian. The initial wave-function is a displaced ground state of a harmonic oscillator. Possible experimental realizations for cold atoms are discussed in detail.

1 Introduction

Collapse and revival phenomena are fascinating and are encountered in a variety of physical situations, that were explored experimentally and theoretically. In the present paper a simple example that can be analyzed analytically, and may be realized experimentally, is presented.

The first collapse and revival phenomenon that was observed and explained theoretically is the Talbot effect [1, 2], where the amplitude of an optical signal collapses and then revives partially and completely. A quantum phenomenon of this type is the quantum carpet [3, 4, 5]. Some revivals discussed here are of different nature than the ones found for the Talbot effect and the quantum carpet. Collapses and revivals, as well as fractional revivals and superrevival structures were observed for wave packets in Rydberg atoms [6, 7, 8, 9, 10, 11, 12, 13]. Also, this phenomenon was observed for interacting bosons [14, 15], and model systems [16, 17, 18, 19, 20]. Similar phenomenon was found for chaotic systems [21]. For the two site Bose Hubbard model, the difference in populations of the two sites exhibits collapses and revivals [22].

A simple model where the phenomenon of collapses and revivals is found is for noninteracting bosons in a weakly anharmonic trap [23]. In this specific situation the particles are prepared in the ground state of the trap and then the potential is instantaneously shifted by some distance. In a harmonic trap, the wave packet oscillates with the frequency of the trap and so do the various

observables, for example, the position x and the momentum p . As a result of the anharmonicity, these oscillations are superimposed by an envelope exhibiting collapses and revivals. Some of our numerical results were presented in [23] that focused on a different issue, namely echoes resulting of the interplay between two displacements. In the present work, analytic formulas for the evolution of the observables are derived.

One should remember that within the model we explore the evolution is coherent and information is not lost even during the collapse. This coherence enables the revivals.

The model presented here is simple and the evolution of the observables is described in a straightforward manner. The simplicity is of great value if used to explore more complex situations. For example, effects of interparticle interactions will result in deviations from our predictions. These can be detected in experiments. The significance of these effects can be tuned by the particle density.

The analytical method we use in the present paper is the semiclassical approximation assuming that the energy level spacing is much smaller than the energy.

When we expand a symmetric potential around its minimum, the leading order is harmonic and the first correction is a term of the form βx^4 . Therefore, we study a model described by the Hamiltonian

$$H' = \frac{p'^2}{2m'} + \frac{1}{2}m'\omega_0'^2 x'^2 + \frac{\beta'}{4}x'^4, \quad (1)$$

In dimensionless units

$$x = x' / \sqrt{\hbar/m'\omega_0'} \quad (2)$$

$$t = \omega_0' t' \quad (3)$$

$$H = \frac{H'}{\hbar\omega_0'} \quad (4)$$

$$p = p' \sqrt{\frac{1}{\hbar m' \omega_0'}}, \quad (5)$$

where prime denotes the corresponding values in physical units, and the Hamiltonian takes the form

$$H = \frac{p^2}{2} + \frac{1}{2}x^2 + \frac{1}{4}\beta x^4, \quad (6)$$

where

$$\beta = \beta' \left(\frac{\hbar}{m'^2 \omega_0'^3} \right). \quad (7)$$

In the present work we assume $\beta \ll 1$. The Schrödinger equation is

$$i\frac{\partial}{\partial t}\psi = H\psi. \quad (8)$$

The model (6) is an idealized model that will be shown to exhibit collapse and revival behavior. This is a very general phenomenon, and therefore it is relevant for a large variety of models. More generally, let us expand eigenenergies around a level \bar{n} [24, 25] in the form

$$E_n \simeq E_{\bar{n}} + E'_{\bar{n}}\delta + \frac{1}{2}E''_{\bar{n}}\delta^2 + \frac{1}{6}E'''_{\bar{n}}\delta^3 \quad (9)$$

where δ is defined by $\delta = n - \bar{n}$, \bar{n} is the state with maximal probability for a displaced ground state of a harmonic oscillator, $E'_{\bar{n}}$, $E''_{\bar{n}}$ and $E'''_{\bar{n}}$ are derivatives of the energy with respect to the quantum number n , calculated at \bar{n} . We consider a situation where the derivatives decrease rapidly with the order, so that

$$E'_{\bar{n}} \gg E''_{\bar{n}} \gg E'''_{\bar{n}}. \quad (10)$$

This is the case for high energy levels n if the level is to a good approximation a power of the quantum number [8]. From condition (10) follows the separation of time scales in the system dynamics.

In Section 2 the dynamics of observables is calculated for the simple model (6) while in Section 3 possible experimental realizations in the field of cold atoms are presented. The results are summarized and discussed in Section 4.

2 Collapse and Revival of the expectation values of position and momentum

In this section we study the expectation values of the position and momentum operators for an initial Gaussian wavepacket displaced by some distance d from the minimum of the potential. For small β the system exhibits collapses and revivals [23]. This phenomenon is explained in terms of the semiclassical approximation using a method similar to the one used in [22]. The phenomenon was found numerically and semianalytically for the system (1) in [23]. Since this phenomenon is expected to take place for high energy levels, where the energy is much larger than the level spacing, we use the semiclassical approximation in the leading order.

It is important to remember that second order in β of the semiclassical approximation is more accurate than second order in perturbation theory for high energy levels. (see detailed discussion in [22]) Using the semiclassical spectrum the evolution of $\langle \hat{x}(t) \rangle$ and $\langle \hat{p}(t) \rangle$ is calculated.

2.1 Energy spectrum calculation using the WKB (Wentzel, Kramers and Brillouin) approximation

In order to use the WKB approximation, we calculate the action integral as

$$\begin{aligned}
I &= \frac{1}{\pi} \int_{-\tilde{a}}^{\tilde{a}} p dx \\
&= \frac{1}{\pi} \int_{-\tilde{a}}^{\tilde{a}} \sqrt{2 \left(E - \frac{1}{2}x^2 - \frac{\beta}{4}x^4 \right)} dx
\end{aligned} \tag{11}$$

where $\pm\tilde{a}$ are the turning points of the path related to the energy by

$$E = \frac{1}{2}\tilde{a}^2 + \frac{\beta}{4}\tilde{a}^4. \tag{12}$$

The integral is calculated to the second order in β and is found to be

$$I = E - \frac{3}{8}\beta E^2 + \frac{35}{64}\beta^2 E^3. \tag{13}$$

This is the value of the action for a fixed value of energy and β . Solving for the energy as function of the action to the second order in β results in

$$E = I + \frac{3}{8}\beta I^2 - \frac{17}{64}\beta^2 I^3. \tag{14}$$

The action is quantized as

$$I_n = n + \frac{1}{2}. \tag{15}$$

Substituting (15) in (14), the energy spectrum of the Hamiltonian to second power of β yields

$$\begin{aligned}
E_n &= \left(n + \frac{1}{2} \right) + \frac{3\beta}{8} \left(n^2 + n + \frac{1}{4} \right) \\
&\quad - \beta^2 \left(\frac{17}{64}n^3 + \frac{51}{128}n^2 + \frac{51}{256}n + \frac{17}{512} \right).
\end{aligned} \tag{16}$$

A slightly different spectrum is obtained by using quantum perturbation theory. Comparison to the exact result obtained by numerical diagonalization of the Hamiltonian (6) shows that the WKB approximation gives a more accurate energy spectrum, for high levels. For $\beta = 1 \cdot 10^{-4}$ (the value used in Fig. 1) the WKB method gives a more accurate result for $n > 4$.

2.2 Explicit calculation of $\langle \hat{x}(t) \rangle$ and $\langle \hat{p}(t) \rangle$

The initial wavefunction is the ground state of the harmonic oscillator $|n=0\rangle$, displaced by d at time $t=0$. The displacement operator is $T(d) = e^{-i\hat{p}d}$. The displacement of the harmonic ground state satisfies [23]

$$\langle m|T(d)|0\rangle = e^{-\frac{\gamma^2}{2}} \frac{\gamma^m}{\sqrt{m!}} = e^{-\frac{\gamma^2}{2}} C_m(\gamma), \quad (17)$$

where

$$\gamma = \frac{d}{\sqrt{2}} \quad (18)$$

and

$$C_n(\gamma) = \frac{\gamma^n}{\sqrt{n!}}. \quad (19)$$

The displaced state is in fact a coherent state of the harmonic oscillator Hamiltonian [26]. We assume that the correction to the harmonic Hamiltonian does not change the eigenstates significantly and therefore use this basis of eigenstates in future calculations.

The wavefunction evolution is given by

$$|\psi(t)\rangle = e^{-\frac{\gamma^2}{2}} \sum_n C_n(\gamma) e^{-iE_n t} |n\rangle \quad (20)$$

and expectation values of the position and momentum operators are

$$\begin{aligned} \langle \hat{x}(t) \rangle &= \langle \psi(t) | \hat{x} | \psi(t) \rangle \\ &= \sqrt{2} \exp(-\gamma^2) \sum_{n=0}^{\infty} [C_n(\gamma) C_{n+1}(\gamma) \sqrt{n+1} \cos((E_{n+1} - E_n)t)] \end{aligned} \quad (21)$$

and

$$\langle \hat{p}(t) \rangle = -\sqrt{2} \exp(-\gamma^2) \sum_n [C_n(\gamma) C_{n+1}(\gamma) \sqrt{n+1} \sin((E_{n+1} - E_n)t)]. \quad (22)$$

The occupation probabilities $|\langle n | \psi \rangle|^2$ satisfy a Poisson distribution whose mean and variance are

$$\bar{n} = \overline{(n - \bar{n})^2} = \gamma^2, \quad (23)$$

where γ satisfies (18). These can be controlled by the initial displacement. Hence, the weight of (21) is concentrated around \bar{n} . Using the expression (19) for C_n one finds

$$\langle \hat{x}(t) \rangle = \sqrt{2} e^{-\gamma^2} \gamma \sum_n \left(\frac{\gamma^{2n}}{n!} \right) \cos((E_{n+1} - E_n)t) \quad (24)$$

and

$$\langle \hat{p}(t) \rangle = -\sqrt{2}e^{-\gamma^2} \gamma \sum_n \left(\frac{\gamma^{2n}}{n!} \right) \sin((E_{n+1} - E_n)t). \quad (25)$$

Expanding to the second order in the deviation from \bar{n} and using the Stirling formula [27] results in

$$\begin{aligned} \langle \hat{x}(t) \rangle &= \frac{1}{\sqrt{\pi}} \sum_n e^{-\frac{1}{2\gamma^2}(n-\bar{n})^2} \cos((E_{n+1} - E_n)t) \\ &= \frac{1}{\sqrt{\pi}} \Re \left(\sum_n e^{-\frac{1}{2\gamma^2}(n-\bar{n})^2} e^{-i(E_{n+1}-E_n)t} \right) \end{aligned} \quad (26)$$

and

$$\begin{aligned} \langle \hat{p}(t) \rangle &= -\frac{1}{\sqrt{\pi}} \sum_n e^{-\frac{1}{2\gamma^2}(n-\bar{n})^2} \sin((E_{n+1} - E_n)t) \\ &= \frac{1}{\sqrt{\pi}} \Im \left(\sum_n e^{-\frac{1}{2\gamma^2}(n-\bar{n})^2} e^{-i(E_{n+1}-E_n)t} \right), \end{aligned} \quad (27)$$

respectively.

From (16) we find

$$\Delta E_n = E_{n+1} - E_n = 1 + \frac{3\beta}{4}(n+1) - \beta^2 \left(\frac{51}{32}n + \frac{51}{64}n^2 + \frac{119}{256} \right). \quad (28)$$

In (26) and (28) it is useful to change to the variable

$$n' = n - \bar{n}. \quad (29)$$

In terms of this variable

$$\Delta E_n = b_0 + b_1 n' + b_2 n'^2, \quad (30)$$

where

$$\begin{aligned} b_0 &= E_{\bar{n}+1} - E_{\bar{n}} \\ &= 1 + \frac{3}{4}\beta(\bar{n}+1) - \beta^2 \left(\frac{119}{256} + \frac{51}{32}\bar{n} + \frac{51}{64}\bar{n}^2 \right), \end{aligned} \quad (31)$$

$$b_1 = \frac{3}{32} (8\beta - 17\beta^2 - 17\bar{n}\beta^2), \quad (32)$$

and

$$b_2 = -\frac{51}{64}\beta^2. \quad (33)$$

It is useful to define the sum

$$\tilde{S}^x = \sum_{n'=-\bar{n}}^{\infty} e^{-\frac{n'^2}{2\gamma^2}} e^{it(b_1 n' + b_2 n'^2)} \quad (34)$$

In this notation,

$$\langle \hat{x}(t) \rangle = \frac{1}{\sqrt{\pi}} \Re \left(e^{-ib_0 t} \tilde{S}^x \right) \quad (35)$$

and

$$\langle \hat{p}(t) \rangle = \frac{1}{\sqrt{\pi}} \Im \left(e^{-ib_0 t} \tilde{S}^x \right). \quad (36)$$

In the leading order in β , we see that the sum (34) exhibits revivals at integer multiples of

$$T_r = \frac{2\pi}{b_1}. \quad (37)$$

Using (31), these are superimposed on the rapid oscillations of period

$$T_{osc} = \frac{2\pi}{b_0}. \quad (38)$$

This period is approximately corresponding to the classical harmonic oscillator period (equals to 2π in our dimensionless units).

In the leading order in β (using (37) and (32))

$$T_r = \frac{8\pi}{3\beta}. \quad (39)$$

We set $t = mT_r + \tau$ around the m^{th} revival, where $-\frac{1}{2}T_r < \tau < \frac{1}{2}T_r$. Hence, the sum (34) can be written in the form

$$\tilde{S}^x = \sum_m \tilde{S}_m^x \quad (40)$$

with

$$\tilde{S}_m^x = \sum_{n'=-\bar{n}}^{\infty} e^{-\frac{n'^2}{2\gamma^2}} e^{i(b_1 \cdot n' + b_2 \cdot n'^2)(mT_r + \tau)}. \quad (41)$$

\tilde{S}_m^x can be approximated by the integral

$$\tilde{S}_m^x = \int_{-\infty}^{\infty} e^{-\frac{n'^2}{2\gamma^2}} e^{i(b_1 \cdot n' \tau + b_2 \cdot n'^2)(mT_r + \tau)} dn'. \quad (42)$$

The reason is that only the terms with small n' contribute substantially to the sum and the differences between adjacent terms in the sum are small, for $\tau \ll T_r$. However, when T_c/T_r is small, the revival is within these time limits, and outside the function equals to zero. The integral (42) is a Gaussian integral calculated using the methods implemented in [22]. The result to the leading order in β is, using (26), (27), (31) and the integrals (42)

$$\langle \hat{x}(t) \rangle = f_{env}(t) \cos \left(\left(1 + \frac{3}{4} \beta (\bar{n} + 1) \right) t \right) \quad (43)$$

and

$$\langle \hat{p}(t) \rangle = -f_{env}(t) \sin \left(\left(1 + \frac{3}{4} \beta (\bar{n} + 1) \right) t \right), \quad (44)$$

where

$$f_{env}(t) = \sqrt{2\gamma} \sum_m e^{-\frac{1}{2} \left(\frac{t - mT_r}{\sigma} \right)^2} \quad (45)$$

and

$$\frac{1}{\sigma} = \gamma b_1 \quad (46)$$

and γ is given by (18).

In the leading order in β the revival time T_r is given by (39). In this order the width σ satisfies

$$\frac{1}{\sigma} = \frac{3}{4} \gamma \beta \quad (47)$$

The collapse time is defined as the time when the envelope $f_{env}(t)$ reaches $1/e$ of its initial value. Therefore it takes the value

$$\begin{aligned} T_c &= \sqrt{2}\sigma \\ &= \frac{T_r}{\sqrt{2\pi}\gamma} \end{aligned} \quad (48)$$

where we used (46) and (37) that are correct to the leading order in β and the next one.

Using (18) we find

$$T_c = \frac{T_r}{\pi d}. \quad (49)$$

The dynamics of $\langle \hat{x}(t) \rangle$ and $\langle \hat{p}(t) \rangle$ exhibit two different time scales. It displays rapid oscillations with period of T_{osc} (38) superimposed by a slowly varying

envelope $f_{env}(t)$. This envelope is a sum of Gaussian functions, separated by time intervals of T_r (37). The collapse time of each Gaussian is T_c of (49).

Fig. 1 shows the collapse and revival of position, calculated numerically and its envelope calculated analytically using (45), T_r of (39) and $1/\sigma$ of (47) for $d = 4$ and $\beta = 1 \cdot 10^{-4}$. We can see good agreement between the numerical and analytical results.

For this small value of β the leading order in β is sufficient to reproduce the exact numerical results to a high degree of accuracy. However, for larger values of β relevant for the experimental realizations presented in Sec. 3 it is instructive to add the next order correction in β . The envelope function takes the form (45) but with

$$\begin{aligned} T_r &\simeq \frac{8\pi}{3\beta \left(1 - \frac{17}{8}\beta - \frac{17}{8}\gamma^2\beta\right)} \\ &\simeq \frac{8\pi}{3\beta} \left(1 + \frac{17}{8}\beta + \frac{17}{8}\gamma^2\beta\right) \end{aligned} \quad (50)$$

and

$$\frac{1}{\sigma} = \frac{3}{4}\gamma\beta \left(1 - \frac{17}{8}\beta - \frac{17}{8}\gamma^2\beta\right), \quad (51)$$

where (32), (18), (37) and (46) were used.

There are also corections of order β^2 to the phases in the sine and cosine functions in (43) and (44), respectively. These are of no special interest.

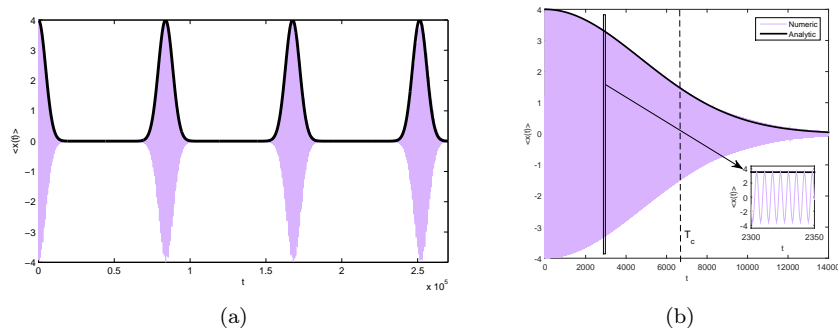


Figure 1: Numerical results based on the solution of the Schrödinger equation with the Hamiltonian (6) (thin purple) and the envelope function f_{env} of (45) (solid black) for $\langle \hat{x}(t) \rangle$ with $\beta = 1 \cdot 10^{-4}$ and $d = 4$: (a) three first revivals (b) zoom-in on the collapse and the fast oscillations

3 Possible experimental realization for cold atoms

In order to observe impressive collapse and revival structures it is required that the collapse time T_c is much shorter than the revival time T_r , and that the revival time is much shorter than the coherence time, namely, the time over which the system is phase coherent.

3.1 Crossed beam trap

In the previous section we assumed the trap to be one dimensional and nearly harmonic, namely, the anharmonic correction is assumed to be small. In order to consider a three dimensional trap effectively one dimensional, it is required that only the ground state of the transverse motion is populated.

Let the direction of the trap and the transverse direction be z and x , respectively. In order to satisfy the quasi-1D condition, the maximal occupied energy in the z direction of the trap must satisfy

$$n \ll n_{max} \quad (52)$$

where

$$n_{max} = \frac{\omega_x}{\omega_z}. \quad (53)$$

ω_z and ω_x are the frequencies of the longitudinal and transverse directions, respectively.

In order to have many available energies in the z direction while the system is still considered one dimensional it is required $\omega_x/\omega_z \gg 1$.

A trap of this type can be realized using perpendicular crossed Gaussian beams resulting in a dipolar trap [28], where the strongly confining beam is along the x axis and the other one is along the z axis.

We turn now to estimate the various quantities for Rubidium. The wavelength of the laser and atomic mass of Rubidium are $\lambda = 1064\text{nm}$ and $m_{Rb} = 1.4432 \cdot 10^{-25}\text{kg}$, respectively. Using cross beam lasers with waists $r_{\parallel} = 18\lambda$, $r_{\perp} = 6\lambda$ and intensities $P_{\perp} = 50\text{W}$ and $P_{\parallel} = 5\text{W}$, one finds $\beta = 3.47 \cdot 10^{-5}$, $\omega_z = 5.36 \cdot 10^4\text{s}^{-1}$, $\omega_x = 1.04 \cdot 10^6\text{s}^{-1}$ and $n_{max} = 19$. This leads to a revival time of $T'_r = 4.37\text{s}$. This revival time can be achieved experimentally. In fact, there may be situations where coherence can be maintained for much longer times [29].

If we require that initially, \bar{n} must satisfy

$$\bar{n} + 3\sqrt{(n - \bar{n})^2} < n_{max}, \quad (54)$$

then $\gamma < 3.11$ (see (23)) and $d < 4.4$.

3.2 Optical lattice potential

Consider a particle moving in the potential

$$V(x') = K'(1 - \cos(qx')) \quad (55)$$

where $q = \frac{2\pi}{\lambda}$.

Assume the time is sufficiently short and K' sufficiently large so that tunneling can be ignored. Then the dynamics can be considered as the one taking place in an anharmonic well discussed in Section 2. For $qx' \ll \frac{\pi}{2}$, this potential is approximated well by

$$V(x') \simeq \frac{1}{2}K'q^2x'^2 - \frac{K'}{4!}q^4x'^4. \quad (56)$$

Therefore, the harmonic part of the potential can be written as

$$\frac{1}{2}m'\omega_0'^2x'^2 = \frac{1}{2}K'q^2x'^2, \quad (57)$$

and hence the frequency of the harmonic oscillator is

$$\omega_0' = \sqrt{\frac{K'}{m'}}q. \quad (58)$$

The anharmonic part is of the form

$$\frac{1}{4}\beta'x'^4 = -\frac{K'}{4!}q^4x'^4 \quad (59)$$

Therefore the anharmonicity coefficient is

$$\beta' = -\frac{K'q^4}{6}. \quad (60)$$

In dimensionless units, the anharmonicity coefficient becomes, using (58) and (7)

$$\beta = -\frac{q\hbar}{6m'^{\frac{1}{2}}K'^{\frac{1}{2}}}. \quad (61)$$

At time $t = 0$ we shift the ground state of a harmonic oscillator laterally by d' so that

$$qd' = \alpha\pi. \quad (62)$$

The displacement cannot be larger than $\frac{\lambda}{4}$, therefore from (62), α should be smaller than 1/2 and takes a value so that (56) describes the potential (55) with little deviation.

Hence, the dimensionless displacement is

$$d = \alpha\pi \frac{(K'm')^{\frac{1}{4}}}{(q\hbar)^{\frac{1}{2}}}. \quad (63)$$

The various time scales in dimensionless units are the classical oscillation

$$T_{osc} = 2\pi, \quad (64)$$

the revival time (see (39))

$$T_r = 16\pi \frac{\sqrt{m'K'}}{q\hbar} \quad (65)$$

and the collapse time (see (49))

$$T_c = \frac{16}{\alpha\pi} \frac{(K'm')^{\frac{1}{4}}}{\sqrt{q\hbar}}. \quad (66)$$

In physical units these are

$$T'_{osc} = \frac{2\pi}{\omega'_0} = \frac{2\pi}{q} \sqrt{\frac{m'}{K'}}, \quad (67)$$

$$T'_r = \frac{T_r}{\omega'_0} = 16\pi \frac{m'}{q^2\hbar} \quad (68)$$

Note that the revival time (68) is independent of strength of the optical potential.

The collapse time is

$$\begin{aligned} T'_c &= \frac{T_c}{\omega'_0} \\ &= \frac{16}{\alpha\pi} \left(\frac{m'^3}{\hbar^2 K' q^6} \right)^{\frac{1}{4}}. \end{aligned} \quad (69)$$

To see the most pronounced collapse and revival picture, we would like to increase the ratio

$$\begin{aligned} \frac{T_r}{T_c} &= \pi d \\ &= \pi^2 \alpha \frac{(K'm')^{\frac{1}{4}}}{(q\hbar)^{\frac{1}{2}}}, \end{aligned} \quad (70)$$

where we used (63).

It is instructive to calculate the various quantities for some representative values of the parameters. Following the parameters of [14], these values are $K' = 35E_r$, $E_r = \frac{\hbar^2 q^2}{2m'}$ is the recoil energy, m' is the mass of a Rubidium atom and $q = \frac{2\pi}{\lambda}$ where $\lambda = 838nm$. For $K' \geq 35E_r$ tunneling between potential wells can be ignored and these can be considered isolated [14].

One should note that the potential in experiment [14] is two dimensional. The numbers are presented here to get a general estimate. We assume here that the motion can be considered decoupled in the two plane directions.

For $\alpha = 0.25$, the various quantities take the values $\beta = 0.0398$, $T_r = 210.3$, $T_c = 41.67$, $T_{osc} = 6.28$, $d = 1.61$, and in physical units $\omega'_0 = 1.719 \cdot 10^5 \frac{1}{sec}$, $T'_r = 1.2msec$, $T'_c = 0.24msec$, $T'_{osc} = 36\mu sec$, $d' = 0.105\mu m$ and

$$K' = 7.581 \cdot 10^{-29} J. \quad (71)$$

In experiments, the optical lattice is typically embedded in a harmonic trap, that is assumed to be modeled by the potential

$$\Delta V = \frac{1}{2} m' \omega'^2_{ext} x'^2, \quad (72)$$

that should be added to the optical potential (55), where $\omega'_{ext} = 2\pi \cdot 60Hz$ as a typical value [14] is relatively small compared to the harmonic part of the optical potential (55) so that $\omega'_{ext} \ll \omega'_0$. The most important effect of the harmonic trap is the shift of the minima of the optical lattice potential given by

$$\frac{d}{dx'} (V + \Delta V) |_{x'_{min,n}} = 0. \quad (73)$$

In the leading order in δ_x , the new minima of the potential are

$$x'_{min,n} = \frac{n\lambda}{2} (1 - \delta_x), \quad (74)$$

where

$$\delta_x = \frac{\omega'^2_{ext}}{\omega'^2_{ext} + \omega'^2_0}. \quad (75)$$

Therefore, the minima are shifted by $\frac{n\lambda}{2}\delta_x$ from the original value $\frac{n\lambda}{2}$, without the confinement.

Since $\omega_{ext} \ll \omega_0$,

$$\delta_x \simeq \left(\frac{\omega'_{ext}}{\omega'_0} \right)^2, \quad (76)$$

therefore δ_x is a small parameter.

The correction to the optical potential for small distances from the center of the well is

$$\Delta V(\Delta x') = \frac{1}{2}m'\omega_0'^2 x_{min,n}'^2 + \frac{1}{2}m'\omega_{ext}'^2 \Delta x'^2 + \frac{1}{6}Kq^4 \left(\frac{n\lambda}{2}\delta_x\right) \Delta x'^3. \quad (77)$$

This is negligible compared to $V(\Delta x')$ since $(\omega'_{ext}/\omega'_0)^2$ and therefore δ_x are extremely small. Moreover, note that $\Delta x'^3$ does not contribute neither to the spectrum nor to the characteristic time scales in the leading order of perturbation theory.

The collapse and revival picture presented in Sec. 2 is very impressive. For realistic parameters collapses and revivals can be observed but the flat regions are much smaller. In Fig. 2 results corresponding to the ones of Fig. 1a are presented for the value K' of (71) as well as for K' increased by a factor of 5 and 10.

We see that as β decreases, the regions where $\langle \hat{x}(t) \rangle$ practically vanishes widen. One should note that the width of the peaks found numerically increases with m due to the blurring effect which occurs as a result of the last term in (28). The correction term of the revival width is of the order of β^4 , hence it could not be estimated in the scope of this work. Therefore, we expect that a better estimate will be found for higher orders in β .

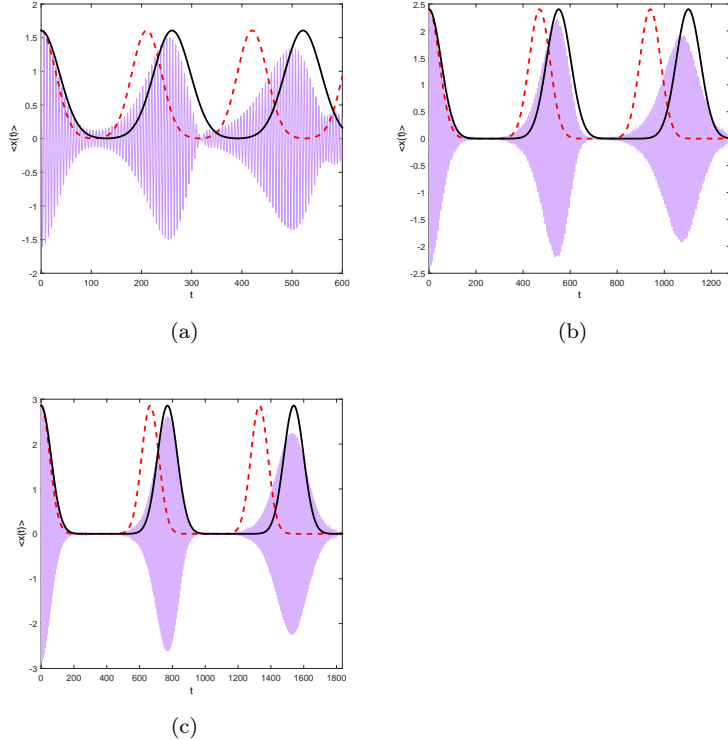


Figure 2: $\langle \hat{x}(t) \rangle$ found numerically as function of time, based on the numerical solution of the Schrödinger equation with the Hamiltonian (6) (thin purple), the analytical envelope predicted by (45) with T_r and σ calculated to the first two leading orders in β using (50) and (51) (solid black) and the envelope predicted by (45) calculated to the leading order in β using (39) and (47) (dashed red) for (a) $K' = 35E_r$, $\beta = 0.0398$ (b) $K' = 175E_r$, $\beta = 0.0178$ (c) $K' = 350E_r$, $\beta = 0.0126$.

The agreement between exact numerical results and approximate analytical results should improve substantially when the next to the leading order is included. The difference between the revival times calculated using (50) and (39) is $\Delta T_r = \frac{17\pi}{3}(1 + \bar{n})$, and $\frac{\Delta T_r}{T_r}$, where T_r is defined by (39), is proportional to β .

4 Summary and Discussion

In this work collapses and revivals were studied for the idealized model of the anharmonic oscillator presented in Sec. 2.

The Hamiltonian

$$H = \frac{1}{2}p^2 + \frac{1}{2}x^2 + \frac{1}{4}\beta x^4 \quad (78)$$

where $\beta \ll 1$, is considered. The initial wavepacket is a ground state of a harmonic oscillator displaced by d and is concentrated around the harmonic eigenstate \bar{n} with variance \bar{n} , where $\bar{n} = \gamma^2$ and $\gamma = \frac{d}{\sqrt{2}}$.

The eigenenergies of this Hamiltonian are expanded around \bar{n} , namely

$$E_n \simeq E_{\bar{n}} + E'_{\bar{n}}(n - \bar{n}) + \frac{1}{2}E''_{\bar{n}}(n - \bar{n})^2 + \frac{1}{6}E'''_{\bar{n}}(n - \bar{n})^3. \quad (79)$$

For the model of this paper this expansion is essentially (30). As can be seen from (31) - (33), it is an expansion in orders of β . For small β , (10) is satisfied, resulting in a separation of time scales given explicitly in what follows. Therefore the simple model studied here is representative of generic systems.

Expectation values of position and momentum are the real and imaginary parts of

$$A(t) = \frac{1}{\sqrt{\pi}} \sum_n e^{-\frac{1}{2\gamma^2}(n-\bar{n})^2} e^{-it(b_0+b_1(n-\bar{n})+b_2(n-\bar{n})^2)}, \quad (80)$$

where b_0 , b_1 and b_2 are defined by (31), (32) and (33), respectively.

The characteristic times are the fast oscillation period, collapse time and revival time are defined as

$$T_{osc} = \frac{2\pi}{b_0}, \quad (81)$$

$$T_c = \frac{\sqrt{2}}{\gamma b_1} \quad (82)$$

and

$$T_r = \frac{2\pi}{b_1}, \quad (83)$$

respectively.

$A(t)$ is a rapidly oscillating function superimposed by an envelope (45). An approximation of this envelope in the leading order in β gives

$$f_{env}(t) = \sqrt{2}\gamma \sum_m e^{-\left(\frac{t-mT_r}{T_c}\right)^2}, \quad (84)$$

where m is the revival number.

The simplicity of the model enabled us to derive analytic formulas (43) and (44) for expectation values of typical observables. These approximate formulas describe very well the exact numerical results, as demonstrated in Fig. 1. In Sec. 3 we demonstrate that the general features that were found for the idealized models hold also for realistic models. Fig. 2 then should be compared to Fig. 1a. There are several systems where one expects to find collapses and revivals as they share the description (9) and (10). Each term in (10) is inversely proportional

to a time scale of the model, hence the different time scales are well separated. The results presented in Sec. 3 show impressive collapse and revival structure that is extremely close to the one shown in Fig. 1.

We hope this work will motivate explorations of experimental realizations that will be as close as possible to the idealized model described by analytical formulas. We focused on realizations in the field of atom optics where significant progress was made in recent years and a high degree of control is possible. An obvious question is : why to do experiments if a good analytical description is available? In such situations one can use the analytical solution to explore the effects of interactions or noise resulting in deviations from the analytical solution.

In summary, collapses and revivals were found for a large variety of systems. In the present paper we presented an idealized model that exhibits this phenomenon, and may enable new directions in its investigation.

5 Acknowledgements

We thank Immanuel Bloch, Steven Tomsovic, Yoav Sagi and Jeff Steinhauer for highly informative and stimulating discussions. This work was supported in part by the Israel Science Foundation (ISF) grants 1028/12 and 931/16, by the US-Israel Binational Science Foundation (BSF) grant number 2010132 and by the Shlomo Kaplansky academic chair. SF thanks the Kavli Institute for Theoretical Physics in Santa Barbara for its hospitality, where this research was supported in part by the US National Science Foundation (NSF) under grant NSF PHY11-25915.

References

- [1] H.F.Talbot, Phil. Mag. 9 (1836).
- [2] L. Rayleigh, Philos. Mag. 11 (1881).
- [3] M.Berry, I.Marzoli, and W.Schleich, Physics World (2001).
- [4] I.Marzoli *et al.*, Acta Physica Slovaca **48**, 323 (1998).
- [5] O.M.Friesch, I.Marzoli, and W.P.Schleich, New J. Phys. **2** (2000).
- [6] J.A.Yeazell, M.Mallalieu, and J. C.R.Stroud, Phys. Rev. Lett. **64** (1989).
- [7] J.A.Yeazell and C.R.Stroud,Jr., Phys. Rev. A **43**, 5153 (1991).
- [8] O.Knospe and R.Schmidt, Phys. Rev. A **54** (1996).
- [9] R.Bluhm and V.A.Kostelecký, Phys. Rev. A **51** (1995).
- [10] I.Sh.Averbukh and N.F.Perel'man, Sov. Phys. Usp **34** (1991).

- [11] I.Sh.Averbukh and N.F.Perelman, Phys. Lett. A **139** (1989).
- [12] I.Sh.Averbukh and N.F.Perel'man, Zh. Eksp. Teor. Fiz **96**, 818 (1989).
- [13] G.Rempe, H.Walter, and N.Klein, Phys. Rev. Lett. **58** (1987).
- [14] M.Greiner, O.Mandel, T.W.Hänsch, and I.Bloch, Nature **419** (2002).
- [15] G.Raithel, W.D.Phillips, and S.L.Rolston, Phys.Rev.Lett. **81**, 3615 (1998).
- [16] E.T.Jaynes and F.W.Cummings, Proc. Inst. Elect. Eng. **51**, 89 (1963).
- [17] J. H. Eberly, N. B. Narozhny, and J. J. Sanchez-Mondragon, Phys. Rev. Lett. **44**, 1323 (1980).
- [18] K.Sakmann, A.I.Streltsov, O.E.Alon, and L.S.Cederbaum, Phys. Rev. A **89**, 023602 (2014).
- [19] A.I.Streltsov, O.E.Alon, and L.S.Cederbaum, Phys. Rev. A **73**, 063626 (2006).
- [20] I.Sh.Averbukh, Phys. Rev. A **46** (1992).
- [21] S.Tomsovic and J.H.Lefebvre, Phys. Rev. Lett. **79**, 3629 (1997).
- [22] H.Veksler and S.Fishman, New. J. Phys. **17**, 053030 (2015).
- [23] M.Herrera, T.M.Antonsen, E.Ott, and S.Fishman, Phys. Rev. A **86**, 023613 (2012).
- [24] R.W.Robinett, Phys. Rep. **392**, 1 (2004).
- [25] R.Bluhm, A.Kostelecký, and J.Porter, Am. J. Phys. **64** (1995).
- [26] A.Messiah, *Quantum Mechanics* (Dover Publications, 1961).
- [27] J. F.Epperson, *An Introduction to Numerical Methods and Analysis* (John Wiley & Sons, 2013).
- [28] R.Grimm, M.Weidemüller, and Y.B.Ovchinnikov, Adv. At. Mol. Opt. Phys. **42**, 95 (2000).
- [29] J.Steinhauser, Private communication.